

**Zeitschrift:** Helvetica Physica Acta  
**Band:** 69 (1996)  
**Heft:** 4

**Artikel:** Probing density fluctuations at low and high redshift  
**Autor:** Lahav, Ofer  
**DOI:** <https://doi.org/10.5169/seals-116958>

#### **Nutzungsbedingungen**

Die ETH-Bibliothek ist die Anbieterin der digitalisierten Zeitschriften auf E-Periodica. Sie besitzt keine Urheberrechte an den Zeitschriften und ist nicht verantwortlich für deren Inhalte. Die Rechte liegen in der Regel bei den Herausgebern beziehungsweise den externen Rechteinhabern. Das Veröffentlichen von Bildern in Print- und Online-Publikationen sowie auf Social Media-Kanälen oder Webseiten ist nur mit vorheriger Genehmigung der Rechteinhaber erlaubt. [Mehr erfahren](#)

#### **Conditions d'utilisation**

L'ETH Library est le fournisseur des revues numérisées. Elle ne détient aucun droit d'auteur sur les revues et n'est pas responsable de leur contenu. En règle générale, les droits sont détenus par les éditeurs ou les détenteurs de droits externes. La reproduction d'images dans des publications imprimées ou en ligne ainsi que sur des canaux de médias sociaux ou des sites web n'est autorisée qu'avec l'accord préalable des détenteurs des droits. [En savoir plus](#)

#### **Terms of use**

The ETH Library is the provider of the digitised journals. It does not own any copyrights to the journals and is not responsible for their content. The rights usually lie with the publishers or the external rights holders. Publishing images in print and online publications, as well as on social media channels or websites, is only permitted with the prior consent of the rights holders. [Find out more](#)

**Download PDF:** 16.01.2026

**ETH-Bibliothek Zürich, E-Periodica, <https://www.e-periodica.ch>**

# Probing Density Fluctuations at Low and High Redshift

By Ofer Lahav

Institute of Astronomy, Madingley Road, Cambridge CB3 0HA, UK

*Abstract* We discuss cosmological inference from galaxy surveys at low and high redshifts. Studies of optical and IRAS redshift surveys with median redshift  $\bar{z} \sim 0.02$  yield measurements of the density parameter  $\Omega$  and the power-spectrum of density fluctuations, but both cannot easily be related to the properties of the underlying mass distribution due to the uncertainty in the way galaxies are biased relative to the mass distribution. Moreover, currently little is known about fluctuations on scales intermediate between local galaxy surveys ( $\sim 100h^{-1}$  Mpc) and the scales probed by COBE ( $\sim 1000h^{-1}$  Mpc). We focus here on several issues, as examples of clustering on different scales: the extent of the Supergalactic Plane, an optimal reconstruction method of the density and velocity fields, the effect of biasing on determination of  $\Omega$  from redshift distortion, the future big surveys SDSS and 2dF (with median redshift  $\bar{z} \sim 0.1$ ) and radio sources and the X-Ray Background as useful probes of the density fluctuations at higher redshift ( $\bar{z} \sim 1$ ).

## 1 Introduction

It is believed by most cosmologists that on the very large scales the universe obeys the equations of General Relativity for an isotropic and homogeneous system, and that the Friedmann-Robertson-Walker (FRW) metric is valid. However, on scales much smaller than the horizon the distribution of luminous matter is clumpy. Galaxy surveys in the last decade have provided a major tool for cosmographical and cosmological studies. In particular, surveys such as CfA, SSRS, IRAS, APM and Las Campanas yielded useful

information on local structure and on the density parameter  $\Omega$  from redshift distortion and from comparison with the peculiar velocity field. Together with measurements of the Cosmic Microwave Background (CMB) radiation and gravitational lensing the redshift surveys provide major probes of the world geometry and the dark matter.

In spite of the rapid progress there are two gaps in our current understanding of the density fluctuations as a function of scale: (i) It is still unclear how to relate the distributions of light and mass, in particular how to match the clustering of galaxies with the CMB fluctuations, (ii) Currently little is known about fluctuations on intermediate scales between these of local galaxy surveys ( $\sim 100h^{-1}$  Mpc) and the scales probed by COBE ( $\sim 1000h^{-1}$  Mpc).

A major unresolved issue is the value of the density parameter  $\Omega$ . Putting together different cosmological observations, the derived values seem to be inconsistent with each other. Taking into account moderate biasing, the redshift and peculiar velocity data on large scales yield  $\Omega \approx 0.3 - 1.5$ , with a trend towards the popular value  $\sim 1$  (e.g. Dekel 1994; Strauss & Willick 1995 for summary of results). On the other hand, the high fraction of baryons in clusters, combined with the baryon density from Big Bang Nucleosynthesis suggests  $\Omega \approx 0.2$  (White et al. 1993). Moreover, an  $\Omega = 1$  universe is also in conflict with a high value of the Hubble constant ( $H_0 \approx 80$  km/sec/Mpc), as in this model the universe turns out to be younger than globular clusters. A way out of these problems was suggested by adding a positive cosmological constant, such that  $\Omega + \lambda = 1$ , to satisfy inflation. But two recent observations argue against  $\lambda > 0$  : the observed frequency of lensed quasars is too small, yielding an upper limit  $\lambda < 0.65$  (e.g. Kochanek 1996 and earlier references therein), and the magnitude-redshift relation for Supernovae type Ia (Perlmutter et al. 1996) is consistent with deceleration parameter  $q_0 = \Omega/2 - \lambda > 0$ . So it seems that at present we are far away from knowing the world geometry and the matter content of the universe. The next decade will see several CMB experiments (COBRAS/SAMBA, MAP, VSA) which promise to determine (in a model-dependent way) the cosmological parameters to within a few percent.

We shall focus here on several issues related to clustering and cosmological parameters: the extent of the Supergalactic Plane, an optimal reconstruction method of the density and velocity fields, the effect of biasing on determination of  $\Omega$  from redshift distortion, the future big surveys (SDSS and 2dF) and radio sources and the X-Ray Background as probes of the density fluctuations at high redshift.

## 2 Cosmological Inference from Redshift Surveys

Redshift surveys have been used in two ways: (i) To study the local cosmography (e.g. clusters, superclusters and voids) and (ii) To infer statistically cosmological parameters such as the density parameter  $\Omega$  and the power-spectrum of density fluctuations  $P(k)$  (i.e. the square of the Fourier components). These issues were reviewed in detail by

Dekel (1994) and Strauss & Willick (1995). Here we shall illustrate these topics with some specific examples: the reconstruction of the Supergalactic Plane (i.e. cosmography) and of the determination of  $\Omega$  (i.e. statistics), with special emphasis on the issue of biasing.

## 2.1 The Supergalactic Plane Revisited

The so-called Supergalactic Plane (SGP) was recognized by de Vaucouleurs (1956) using the Shapley-Ames catalogue, following an earlier analysis of radial velocities of nearby galaxies which suggested a differential rotation of the ‘metagalaxy’ by Vera Rubin. This remarkable feature in the distribution of nebulae was in fact already noticed by William Herschel more than 200 years ago. Tully (1986) claimed the flattened distribution of clusters extends across a diameter of  $\sim 0.1c$  with axial ratios of 4:2:1. Shaver & Pierre (1989) found that radio galaxies are more strongly concentrated to the SGP than are optical galaxies, and that the SGP as represented by radio galaxies extends out to redshift  $z \sim 0.02$ . Traditionally the Virgo cluster was regarded as the centre of the Supergalaxy, and this was termed the ‘Local Supercluster’. But recent maps of the local universe indicate that much larger clusters, such as the Great Attractor and Perseus-Pisces on opposite sides of the Local Group are also major components of this planar structure. Supergalactic coordinates are commonly used in extragalactic studies, but the degree of linearity, extent and direction of the SGP have been little quantified in recent years. Moreover, it is important to compare the extent of the SGP with other filamentary structures seen in redshift surveys and in  $N$ -body simulations. Top-down structure formation scenarios (e.g. Hot Dark Matter) in particular predict the formation of Zeldovich pancakes, although these are also seen in hierarchical (bottom-up) scenarios (e.g. Cold Dark Matter).

The Optical Redshift Survey (ORS, Santiago et al. 1995) and the IRAS 1.2Jy survey (Fisher et al. 1995a) have been used recently to revisit the SGP feature (Lahav et al., in preparation). To estimate objectively the extent of the SGP, let us consider a slab embedded in a uniform sphere of radius  $R$  and then construct the ‘moment of inertia tensor’ for the *fluctuation* in the density field:

$$\tilde{C}_{ij} = \frac{1}{V} \sum_{gal} w_{gal} (x_i - \bar{x}_i)(x_j - \bar{x}_j) - \delta_{ij}^K \frac{n_{bg}}{\langle n \rangle} \frac{R^2}{5}, \quad (1)$$

where  $V$  is the volume of the sphere, and  $w_{gal}$  is the weight per galaxy, which corrects for the radial and angular selection functions of the catalogues.  $x_i, x_j$  ( $i, j = 1, 2, 3$ ) are Cartesian components of  $\mathbf{x}$ ,  $n_{bg}$  is the *background* density in the absence of the slab, and  $\langle n \rangle$  the mean density (*including* the slab). The last term is due to a uniform distribution with density  $n_{bg}$ . By diagonalising the moment of inertia it is found that the angle between the normal to the standard SGP and the normal to our objectively identified plane is  $\theta_z \approx 30^\circ$  out to  $R = 8000$  km/sec. The probability of these normals to be within an angle  $\theta_z$  by chance is  $P(< \theta_z) = 1 - \cos(\theta_z)$ , i.e.  $\sim 13\%$ . Unlike the eigen-vectors, the eigen-values of eq. (1), which correspond to the square of the ‘ellipsoid’ axes, depend on the uncertain background density  $n_{bg}$ . Preliminary analysis shows that the SGX and SGY dimensions

are indeed much larger than SGZ, and they extend out radius of at least 6000 km/sec. It is a challenge for any cosmological model to reproduce such a large pancake feature.

It is worth noting that one source of uncertainty in quantifying the connectivity of the SGP is that disk of the Milky Way obscures about 20% of the optical extragalactic sky, this is the so-called “Zone of Avoidance” (ZOA). The ZOA is nearly perpendicular to the SGP. Galaxies behind the ZOA are difficult to detect due to extinction by dust and gas at optical wavelengths, and confusion with Galactic stars. But they can be detected in emission at 21cm by neutral atomic hydrogen (HI). Recent discoveries of galaxies hidden behind the ZOA include the Sagittarius dwarf (Ibata, Gilmore and Irwin 1994), Dwingeloo1 (Kraan-Korteweg et al. 1994) and the cluster A3627 (Kraan-Korteweg et al. 1996), which is possibly at the centre of the Great Attractor region.

## 2.2 Wiener Reconstruction of IRAS

Apart from the ZOA, two other major problems affect most analyses of redshift surveys: shot noise and redshift distortion. One approach to deal with both is Wiener filtering (Fisher et al 1995b). Let us expand the density field  $\rho(\mathbf{r}) = [\mathbf{1} + \delta(\mathbf{r})]\bar{\rho}$  in spherical harmonics and radial Bessel functions:

$$\rho(\mathbf{r}) = \sum_l \sum_m \sum_n C_{ln} \rho_{lmn} j_l(k_n r) Y_{lm}(\hat{\mathbf{r}}), \quad (2)$$

where the  $k_n$ 's are chosen e.g. to satisfy the boundary condition that the logarithmic derivative of the potential is continuous at  $r = R_{max}$ . An estimator of the coefficients from the redshift data is

$$\rho_{lmn}^S = \sum_{gal} \frac{1}{\phi(s)} j_l(k_n s) Y_{lm}^*(\hat{\mathbf{r}}), \quad (3)$$

where  $\phi(s)$  is the radial selection function. Fisher et al. (1995b) showed that the real-space coefficients of the fluctuations can be reconstructed by

$$\delta_{lmn}^R = \sum_{n'n''} \left( \mathbf{S}_1 [\mathbf{S}_1 + \mathbf{N}_1]^{-1} \right)_{nn'} (\mathbf{Z}_1^{-1})_{n'n''} \delta_{lmn''}^S, \quad (4)$$

where the matrix  $\mathbf{Z}_1$  (which depends on the assumed combination of density and biasing parameters,  $\beta = \Omega^{0.6}/b$ ) converts the redshift space coefficients to real space coefficients.  $\mathbf{S}_1 [\mathbf{S}_1 + \mathbf{N}_1]^{-1}$  is the Wiener matrix, roughly representing signal/(signal+noise), which filters the data where they are noisy. The signal matrix  $\mathbf{S}_1$  depends on the assumed prior power-spectrum of fluctuations. It can be shown that this gives the optimal reconstruction in the minimum variance sense, and it can also be derived from Bayesian arguments and Gaussian probability distribution functions. In this approach the density field goes to the mean density at large distances. This does not mean necessarily that the density field

itself disappears at large distances, it only reflects our ignorance on what exists far away, where the data are very poor.

Webster, Lahav & Fisher (1996) have utilised this method to recover the density and velocity fields from the IRAS 1.2Jy redshift survey. Many known structures are seen in the reconstructed maps, including clear confirmations of the clusters N1600 and A3627. The Perseus-Pisces supercluster appears to extend out to roughly 9000 km/sec, and the reconstruction shows 'backside infall' to the Centaurus/Great Attractor region. The Wiener reconstruction of the density field is also the optimal reconstruction (in the minimum variance sense) of any quantity which is linear in the density contrast such as the dipole, bulk flows and the SGP. The misalignment angle between the IRAS and CMB Local Group dipoles is only 13 degrees out to 5000 km/sec, but increases to 25 degrees out to 20,000 km/sec (see Figure 1). It still has to be understood if this misalignment is due to non-linear effects or missing gravity due to the ZOA, power on large scales and/or biasing. The reconstructed IRAS bulk flow out to 5000 km/sec is roughly 300 km/sec (for  $\beta = 0.7$ ), similar in amplitude to that derived from the Mark III peculiar velocities (370 km/sec). However, the two bulk flow vectors deviate by 70 degrees. Finally, a moment of inertia analysis shows that the Wiener reconstructed SGP is aligned within 30 degrees of that defined by de Vaucouleurs, in agreement with the analysis discussed in the previous section.

### 3 $\Omega$ and Bias Parameter from Redshift Distortion

In the previous section we used IRAS galaxies to represent the sources of gravity in the local universe. However, it is most likely that luminous galaxies do not trace perfectly the mass distribution. This effect is commonly phrased as 'biasing', although there is some confusion (or over-simplicity) in modelling it. Kaiser (1984) formulated biasing in terms of statistics of peaks. He showed that in the linear approximation the correlation function of galaxies is related to the mass correlation function by

$$\xi_{gg} = b^2 \xi_{mm} \quad (5)$$

where  $b$  is the 'bias parameter'. It has become a common practice to assume that the galaxy and mass density fluctuations at any point are related by

$$\delta_g = b\delta_m \quad (6)$$

Clearly, if eq. (6) is true then eq. (5) follows, but the reverse is not true. Usually, eq. (6) is assumed in different statistics, but if it does not hold (which is very likely the case), then one compares 'apples and oranges' in the various determinations of  $\Omega$ .

An illustration that biasing can be more complicated than eq. (6) is given when the clustering properties of different galaxy morphologies are compared. For example, Hermit et al. (1996) found that the relative bias factor between early type galaxies and late-types

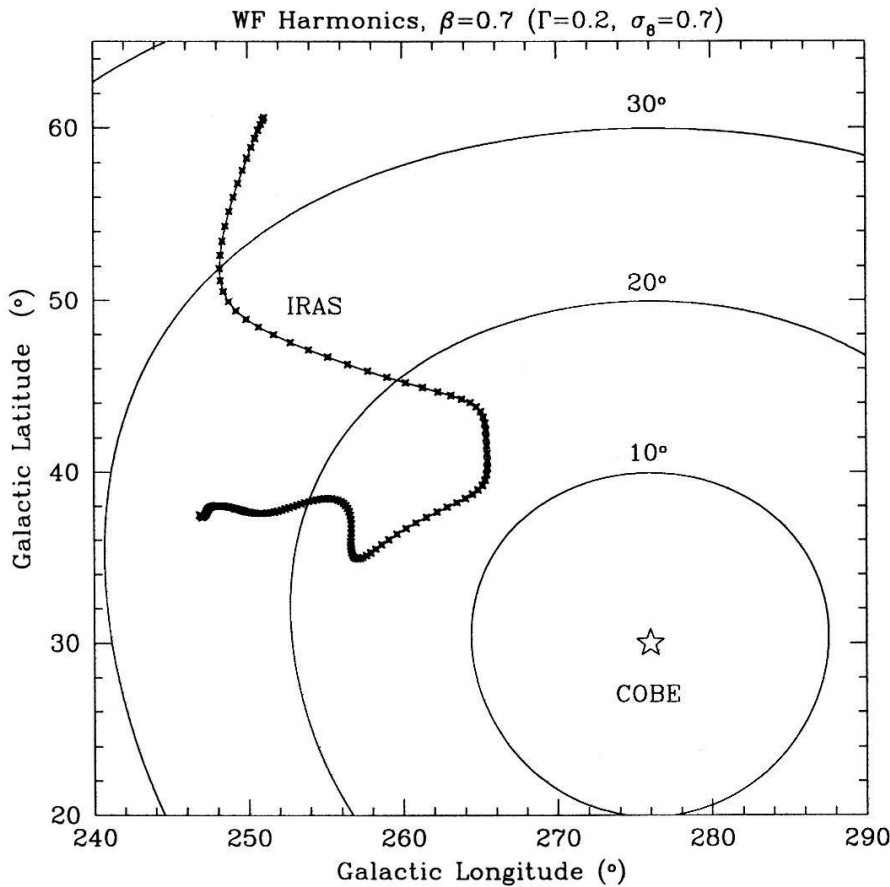


**Fig. 1.** The direction of the Wiener reconstructed IRAS dipole compared with the COBE dipole (in the Local Group frame). The reconstruction assumes the observed power-spectrum of IRAS galaxies (characterized by  $\Gamma$  and  $\sigma_8$ ) and  $\beta = \Omega^{0.6}/b = 0.7$ . The crosses show the convergence of the direction of the reconstructed IRAS dipole. Starting at the top of the plot, the crosses give the direction (in Galactic coordinates) of the dipole within radius  $R$  (in steps of  $1 h^{-1}$  Mpc). The circular curves denote separations from the COBE result in  $10^\circ$  intervals. From Webster, Lahav & Fisher (1996)

weakly depends on scale out to  $10 h^{-1}$  Mpc. On the other hand, on much larger scales voids seem empty for all known galaxy populations. It is therefore crucial to generalize eq. (6) for more realistic scenarios. Many extensions for biasing are possible: non-linear, non-local, scale-dependent, epoch-dependent and stochastic (Dekel & Lahav, in preparation). Here we give a specific example on how the determination of  $\Omega$  from redshift distortion could be modified.

### 3.1 Biasing in Redshift Distortion

Studies of redshift distortion in galaxy redshift surveys aim at deducing  $\beta = \Omega^{0.6}/b$ . Derived values by this method cover the range  $0.45 < \beta < 1.10$  (Strauss & Willick 1995). However, the galaxies play two roles in such analysis: they are both luminous tracers of the mass distribution as well as test particles of the velocity field, and hence the form of biasing is more complicated.

Kaiser (1987) showed that in linear theory and in the far field approximation the

density fluctuation in galaxies in redshift space  $\delta_{g,S}$  is related to the one in real space  $\delta_{g,R}$  by

$$\delta_{g,S} = \delta_{g,R} - \frac{dU}{dr} \quad (7)$$

where  $\frac{dU}{dr} = -\mu^2 \Omega^{0.6} \delta_m$  is the gradient of line of sight velocity in linear theory and  $\mu$  is the cosine of the angle between the line of sight and the  $\mathbf{k}$  vector. We then find that the power spectrum in redshift space is:

$$P_{gg}^S(k) = P_{gg}^R(k) + 2P_{mg}^R(k)\Omega^{0.6}\mu^2 + \Omega^{1.2}\mu^4 P_{mm}^R(k) \quad (8)$$

where  $P_{gg}^R(k)$ ,  $P_{mg}^R(k)$  and  $P_{mm}^R(k)$  are the galaxy-galaxy, mass-galaxy and mass-mass power spectra in real space. This generalizes eq. (3.5) of Kaiser (1987). Only if  $P_{gg}^R(k) = b^2 P_{mm}^R(k)$  and  $P_{gg}^R(k) = bP_{mg}^R$  the relation goes back to the simple and much-used relation:

$$P_{gg}^S(k) = P_{gg}^R(k)(1 + \beta\mu^2)^2. \quad (9)$$

Similarly, the spherical harmonic analysis for redshift distortion in linear theory for a flux-limited survey (Fisher, Scharf & Lahav 1994; eq. 11) can be extended to give for the the mean-square predicted harmonics:

$$\langle |a_{lm}^S|^2 \rangle = \frac{2}{\pi} \int dk k^2 \{ P_{gg}^R(k) |\Psi_l^R(k)|^2 + 2\Omega^{0.6} P_{mg}^R(k) |\Psi_l^R(k)\Psi_l^C(k)| + \Omega^{1.2} P_{mm}^R(k) |\Psi_l^C(k)|^2 \} \quad (10)$$

where  $\Psi_l^R(k)$  and  $\Psi_l^C(k)$  are the real space and redshift correction window functions which depend on the selection and weighting functions. We see that if the density fields of mass and light do not obey linear biasing then direct comparison with  $\beta$  derived by other methods is inconsistent. Better modelling of biasing may help resolving the discrepancies between the different values obtained for  $\Omega$ .

## 4 Future Redshift Surveys: SDSS and 2dF

Existing optical and IRAS redshift surveys contain 10,000-20,000 galaxies. A major step forward using multifibre technology will allow in the near future to produce redshift surveys of millions of galaxies. In particular, there are two major surveys on the horizon. The American-Japanese Sloan Digital Sky Survey (SDSS) will yield images in 5 colours for 50 million galaxies, and redshifts for about 1 million galaxies over a quarter of the sky (Gunn and Weinberg 1995). It will be carried out using a dedicated 2.5m telescope in New Mexico. The median redshift of the survey is  $z \sim 0.1$ . A complementary Anglo-Australian survey, the 2 degree Field (2dF), will produce redshifts for 250,000 galaxies brighter than  $b_J = 19.5^m$  (with median redshift of  $z \sim 0.1$ ), selected from the APM catalogue. The survey will utilize a new 400-fibre system on the 4m AAT, covering  $\sim 1,700$  sq deg of the

sky. About 250,000 spectra will be measured over  $\sim 100$  nights. A deeper extension down to  $R = 21$  for 10,000 galaxies is also planned for the 2dF survey. These surveys will probe scales larger than  $\sim 30h^{-1}$  Mpc. It will also allow accurate determination of  $\Omega$  and bias parameter from redshift distortion. Surveys like 2dF and SDSS will produce unusually large numbers of galaxy spectra, providing an important probe of the intrinsic galaxy properties, for studying e.g. the density-morphology relation. Several groups (e.g. Connolly et al. 1995 ; Sodré & Cuevas 1996; Folkes, Lahav & Maddox 1996) recently devised techniques for automated spectral classification of galaxies. These techniques include e.g. Principal Component Analysis and Artificial Neural Networks.

## 5 Probes of density fluctuations at high redshift

The big new surveys (SDSS, 2dF) will only probe a median redshift  $\bar{z} \sim 0.1$ . It is still crucial to probe the density fluctuations at higher  $z$ , and to fill in the gap between scales probed by previous local galaxy surveys and the scales probed by COBE and other CMB experiments. Here we discuss the X-ray Background (XRB) and radio sources as probes of the density fluctuations at median redshift  $z \sim 1$ . Other possible high-redshift traces are quasars and clusters of galaxies. For review on the evolution of galaxies with redshift see e.g. Fukugita, Hogan & Peebles (1996).

### 5.1 The X-ray Background

Although discovered in 1962, the origin of the X-ray Background (XRB) is still unknown, but is likely to be due to sources at high redshift (for review see Boldt 1987; Fabian & Barcons 1992). Here we shall not attempt to speculate on the nature of the XRB sources. Instead, we *utilise* the XRB as a probe of the density fluctuations at high redshift. The XRB sources are probably located at redshift  $z < 5$ , making them convenient tracers of the mass distribution on scales intermediate between those in the CMB as probed by COBE, and those probed by optical and IRAS redshift surveys (see Figure 2). In terms of the level of anisotropy, the XRB is also intermediate between the tiny CMB fluctuations ( $\sim 10^{-5}$  on angular scales of degrees) and galaxy density fluctuations (of the order of unity on scale of  $8 h^{-1}$  Mpc).

The preliminary measurements of the dipole anisotropy in the XRB (Shafer 1983) were discussed qualitatively (e.g. Rees 1979) by associating it with local clusters such as Virgo and the Great Attractor and by other cosmographical arguments. Lahav, Piran & Treier (1996) recently treated the problem in a statistical rather than cosmographical way. They predicted rms spherical harmonics in the framework of growth of structure by gravitational instability from density fluctuations drawn from a Gaussian random field. The XRB

harmonics are expressed in terms of the power-spectrum of density fluctuations and for evolution scenarios which are consistent with recent measurements of galaxy clustering and the CMB. The dipole is due to large scale structure as well as to the observer's motion (the Compton-Getting effect). For a typical observer the two effects turn out to be comparable in amplitude. The coupling of the two effects makes it difficult to use the XRB for independent confirmation of the CMB dipole being due to the observer's motion. The large scale structure dipole (rms per component) relative to the monopole is in the range  $a_{1m}/a_{00} \sim (0.5 - 9.0) \times 10^{-3}$ . The spread is mainly due to the assumed redshift evolution scenarios of the X-ray volume emissivity  $\rho_x(z)$ . The dipole's prediction is consistent with a measured dipole in the HEAO1 XRB map. Typically, the harmonic spectrum drops with  $l$  like  $a_{lm} \sim l^{-0.4}$ . This behaviour allows us to discriminate a true clustering signal against the flux shot noise, which is constant with  $l$ , and may dominate the signal unless bright resolved sources are removed from the XRB map. The Sachs-Wolfe and Doppler (due to the motion of the sources) effects in the XRB are negligible. Measurements of the spherical harmonic spectrum in maps such as HEAO1 and ROSAT could provide important constraints on amount of clustering at high redshift.

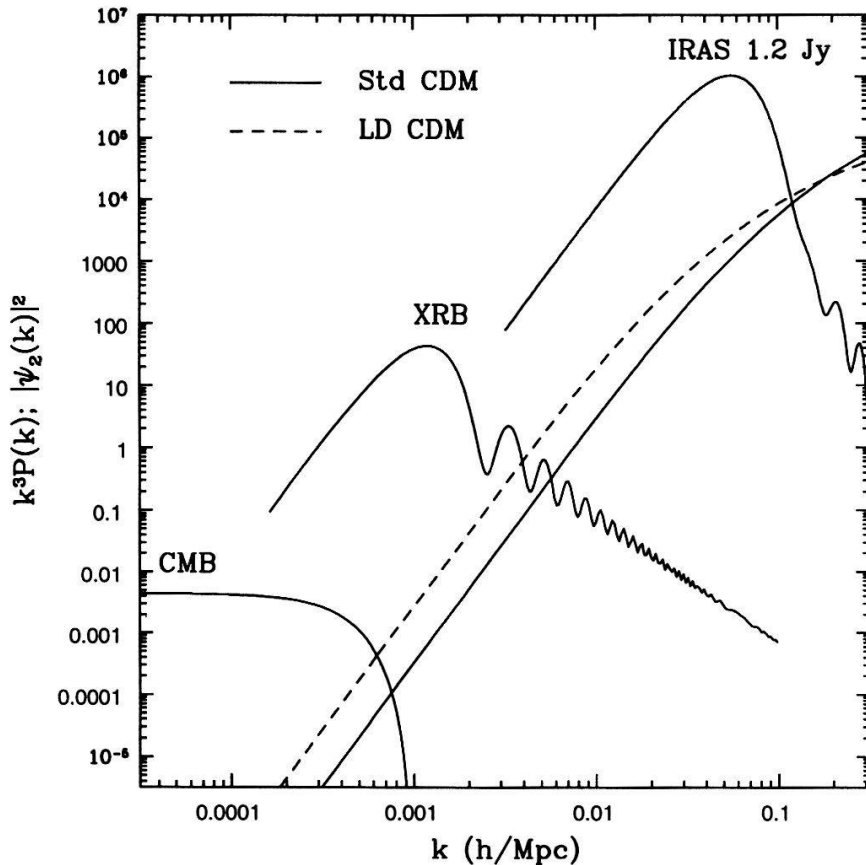


**Fig. 2.** The quadrupole ( $l = 2$ ) 'window functions' in Fourier space for the CMB (Sachs-Wolfe effect), the X-ray Background (for specific model parameters), and IRAS galaxies. The height of the window functions is arbitrary. The solid and dashed lines represent  $k^3 P(k) \sim (\delta\rho/\rho)^2$  for standard Cold Dark Matter model and the observed galaxy power spectrum (fitted by low density CDM model), respectively. From Lahav, Piran & Treyer (1996).

## 5.2 Radio Sources

Surveys of radio sources have typically median redshift  $\bar{z} \sim 1$ , and hence are useful probes of clustering at high redshift. Unfortunately, it is difficult to obtain distance information from these surveys: the radio luminosity function is very broad, and it is difficult to obtain optical redshifts of the radio sources.

Several groups (Kooiman et al 1995, Sicotte 1995, Loan, Wall and Lahav 1996, Cress et al. 1996) have recently studied clustering of radio sources. For example, Loan et al. (1996) measured the angular two-point correlation function  $w(\theta)$  in the Green Bank and Parkes-MIT-NRAO 4.85 GHz surveys. The signal is noisy, but with an assumed redshift distribution indicates strong clustering in 3 dimensions. It is convenient to parameterize the evolution of the spatial correlation function in comoving coordinates as:

$$\xi(r_c, z) = (r_c/r_0)^{-\gamma} (1+z)^{\gamma-(3+\epsilon)}. \quad (11)$$

For  $\gamma = 1.8$ , and ‘stable clustering’ ( $\epsilon = 0$ ) the derived correlation length is  $r_0 \approx 18h^{-1}$  Mpc, larger than the value for nearby normal galaxies and comparable to the cluster-cluster correlation length. This may suggest that radio sources are associated with high-density regions. This is in accord with earlier studies (Bahcall & Chokshi 1992, Peacock & Nicholson 1991) and the new studies mentioned above. It is of interest to detect the dipole and higher harmonics in these radio surveys. As for the XRB, it is found that the motion (Ellis & Baldwin 1984) and large scale structure dipole effects are comparable (Baleisis 1996), but both are smaller than the shot noise. New surveys, such as FIRST and NVSS will constrain much better the clustering properties at high redshift.

## 6 Discussion

We have shown some recent studies of galaxy surveys, and their cosmological implications. Local IRAS and optical surveys have been used to describe the local cosmography (e.g. the Supergalactic Plane) and to constrain  $\Omega$  (e.g. from redshift distortion and dipoles). However, the issue of biasing is still conceptually underdeveloped, and is crucial for analysing the new big surveys (2dF, SDSS). To study galaxy evolution and the validity of the FRW metric on large scales it is important to explore density fluctuations at higher redshift. The examples of the X-ray Background and radio sources are encouraging, but redshift information is required to constrain the growth of cosmic structure with time. With the dramatic increase of data, we should soon be able to map the fluctuations with scale and epoch.

**Acknowledgments** I thank my collaborators for their contribution to the work presented here, and for stimulating discussions, and the organizers of JR96 for an enjoyable meeting.

## References

- [1] Bahcall N.A. & Chokshi, A., 1992, ApJ, 382, L33
- [2] Baleisis A., 1996, M.Phil. thesis, Cambridge University
- [3] Boldt E., 1987, Phys. Reports, 146, 215
- [4] Connolly, A.J., Szalay, A.S., Bershady, M.A., Kinney, A.L. & Calzetti, D. 1995, AJ, 110, 1071
- [5] Cress C.M., Helfand D.J., Becker R.H., Gregg M.D., White R.L., 1996, ApJ, in press
- [6] Dekel, A., 1994, ARA&A, 32, 371
- [7] de Vaucouleurs, G., 1956, Vistas in Astronmy, 2, 1584
- [8] Ellis, G.F.R. & Baldwin, J.E. 1984, MNRAS, 206, 377
- [9] Fabian A.C. & Barcons X., 1992, ARA&A, 30, 429
- [10] Fisher, K.B., Scharf, C.A. & Lahav, O., 1994, 266, 219
- [11] Fisher, K.B., Huchra, J.P., Davis, M., Strauss, M.A., Yahil, A., & Schlegel, D. 1995a, ApJS, 100, 69
- [12] Fisher, K.B., Lahav, O., Hoffman, Y., Lynden-Bell, D., & Zaroubi, S. 1995b, MNRAS, 272, 885
- [13] Folkes, S., Lahav, O. & Maddox, S.J., 1996, MNRAS, in press
- [14] Fukugita, M., Hogan, C.J. & Peebles, P.J.E., 1996, Nature, 381, 489
- [15] Gunn, J.E. & Weinberg, D.H., 1995, in *Wide-Field Spectroscopy and the Distant Universe*, eds. S.J. Maddox & A. Aragon-Salamanca, World Scientific, Singapore
- [16] Hermit, S. Santiago, B.X., Lahav, O., Strauss, M.A., Davis, M., Dressler, A., & Huchra, J.P., 1996, MNRAS, in press
- [17] Ibata, R.A., Gilmore, G. & Irwin, M.J., 1994, Nature, 370, 1941
- [18] Kaiser, N., 1984, ApJ, 284, L9
- [19] Kaiser, N., 1987, MNRAS, 227, 1
- [20] Kochanek, C.S., 1996, ApJ, 466, 638
- [21] Kooiman B.L., Burns J.O., Klypin A.A., 1995, ApJ, 448, 500
- [22] Kraan-Korteweg, R.C., Loan, A.J., Burton, W.B., Lahav, O., Ferguson, H.C., Henning, P.A., & Lynden-Bell, D., 1994, Nature, 372, 77
- [23] Kraan-Korteweg, R.C., Woudt, P.A., Cayatte, V., Fairall, A.P., Balkowski, C. & Henning, P.A., 1996, Nature, 379, 519
- [24] Lahav, O., Piran, T. & Treyer M.A., 1996, MNRAS, in press

- [25] Loan, A.J., Wall, J.V. & Lahav, O., 1996, MNRAS, submitted
- [26] Peacock J.A & Nicholson D., 1991, MNRAS, 253, 307
- [27] Perlmutter, S., et al., 1996, preprint
- [28] Rees, M.J., 1979, *Objects of High Redshifts*, IAU Symp., G. Abell & J. Peebles Eds.
- [29] Santiago, B.X., Strauss, M.A., Lahav, O., Davis, M., Dressler, A., & Huchra, J.P. 1995, ApJ, 446, 457
- [30] Shafer, R.A., 1983, PhD Thesis, University of Maryland, NASA TM-85029
- [31] Shaver, P.A., & Pierre, M., 1989, A&A, 220, 35
- [32] Sicotte H., 1995, Ph.D. thesis, Princeton University
- [33] Sodré L. Jr. & Cuevas, H., 1996, MNRAS, submitted
- [34] Strauss, M.A. & Willick, J.A. 1995, Phys. Reports, 261, 271
- [35] Tully, B.R., 1986, ApJ, 303, 25
- [36] Webster, A.M., Lahav, O. & Fisher, K.B., 1996, MNRAS, submitted
- [37] White, S.D.M., Navarro, J.F., Evrard, A.E. & Frenk, C.S., 1993, Nature, 366, 429